Magnetic study of $PrFe_2Si_2$ and $PrFe_2Ge_2$ compounds by susceptibility measurements, neutron diffraction, and Mössbauer spectroscopy

B. Malaman and G. Venturini
Laboratoire de Chimie du Solide Minéral, Université de Nancy I, Boîte Postale 239, 54506 Vandoeuvre-les-Nancy CEDEX, France

A. Blaise and J. P. Sanchez
Centre d'Etudes Nucléaires de Grenoble, Département de Recherche Fondamentale sur la Matière Condensée, 85X, 38041 Grenoble CEDEX, France

G. Amoretti
Dipartimento di Fisica, Universita di Parma, I-43100 Parma, Italy

(Received 8 September 1992)

The magnetic properties of the tetragonal ($ThCr_2Si_2$- type) $PrFe_2X_2$ (X =Si,Ge) compounds have been investigated using magnetization, neutron-diffraction and ^{57}Fe-Mössbauer-spectroscopy measurements. $PrFe_2Si_2$ and $PrFe_2Ge_2$ were shown to order antiferromagnetically (AF) at 7.70 and 14.2 K, respectively. Neutron and Mössbauer transferred-fields data indicate the occurrence of a type-II AF structure (++--) with the moment aligned along the c axis in both compounds but with quite different saturation moments: 1.41 (Si) and 2.75μ_B (Ge) at 1.3 K. In addition, $PrFe_2Ge_2$ presents a transition towards an incommensurate modulated structure at 9 K. The results are discussed in the frame of a crystal-field model.

I. INTRODUCTION

The ternary rare-earth RT_2X_2 compounds (R =rare-earth, T =3d, 4d, or 5d transition metal, and X =Si, Ge) were shown to exhibit exciting properties ranging from superconductivity to heavy fermion behavior.[1-3] Most of them crystallize in the body-centered tetragonal structure of the $ThCr_2Si_2$-type (space group $I4/mmm$) in which the R(Th), T(Cr), and X(Si) atoms occupy the 2(a), 4(d), and 4(e) sites, respectively. The atoms are arranged in planes stacked perpendicular to the c axis with the sequence R-X-T-X-R (Fig. 1). It has been reported that none of these compounds carry any magnetic moment on the T atom, except for the RMn_2X_2 compounds. These intermetallics usually order magnetically at low temperatures (due to the ordering of the R sublattice) and present different types of magnetic structures.

The magnetic properties of $PrFe_2X_2$ compounds have been studied extensively by magnetization[4,5] and neutron-diffraction measurements.[5-7] $PrFe_2Ge_2$ is a collinear antiferromagnet (++--) below 13 K of the same kind as $NdFe_2Si_2$.[6-8] In addition, $PrFe_2Ge_2$ presents a transition towards an incommensurate modulated structure between 9 and 13 K.[7] $PrFe_2Si_2$ was studied by Felner and co-workers.[4] According to their results, no magnetic ordering was observed on the Pr sublattice down to 1.5 K.

In this paper, we report on an extensive study of the magnetic structures of $PrFe_2Si_2$ and $PrFe_2Ge_2$ compounds, using magnetization, neutron-diffraction and ^{57}Fe-Mössbauer-spectroscopy measurements. The results are discussed in the frame of a crystal-field model. Comparison between the $PrFe_2Si_2$ and $PrFe_2Ge_2$ compounds and a general discussion are given in conclusion.

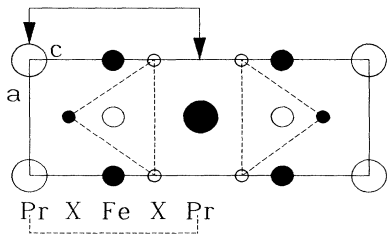

FIG. 1. Crystal structure of $PrFe_2X_2$ ($ThCr_2Si_2$ structure type) compounds projected along the b axis. The solid circles represent atoms at $y=\frac{1}{2}$, whereas open circles stand for atoms at $y=0$.

II. EXPERIMENTAL PROCEDURES

$PrFe_2Si_2$ and $PrFe_2Ge_2$ were prepared from commercially available high-purity elements. Pellets of stoichiometric mixture were compacted using a steel die and then introduced into silica tubes sealed under argon (100 mm Hg). First, the samples were gradually heated to 1073 K for preliminary homogenization treatment and then melted in an induction furnace. The resulting ingots were annealed for 5 days at 1173 K. Purity of the final product was checked by powder x-ray-diffraction technique, using a Guinier camera (Cu-Kα). Lattice parameters at room temperature (Table I) are in good agreement with earlier published values.[4,9]

We performed magnetic measurements in field up to 5 T on both compounds, using a superconducting quantum

TABLE I. $PrFe_2X_2$ compounds (X = Si, Ge): Main crystallographic parameters.

Crystallographic data (300 K)					
Compounds	a (Å)	c (Å)	c/a	V (Å^3)	References
$PrFe_2Si_2$	4.0073(8)	10.054(1)	2.509	161.4	This work
	3.975(3)	10.016(8)	2.520	158.2	9
	4.018(5)	10.06(5)	2.504	162.4	4
$PrFe_2Ge_2$	4.0573(5)	10.517(1)	2.592	173.1	This work
	4.060(2)	10.508(5)	2.588	173.2	9

interference device (SQUID) magnetometer. The samples in powder form were measured in the temperature range 4.2–300 K.

Neutron-diffraction experiments were carried out at the Institut Laüe Langevin (ILL), Grenoble. The diffraction patterns were recorded using the one-dimension curved multidetector D1b at a wavelength $\lambda = 2.5293$ Å. Several patterns were collected between 1.3 and 300 K and special attention was paid to the 1.3–16 K temperature range where 16 patterns (i.e., 1 K step) were recorded. The first refinements, carried out with the neutron patterns recorded at room temperature, pointed to the occurrence of texture effects (due to tablet-like crystallites, the c axis taking a preferential orientation perpendicular to the neutron beam). In order to correct this effect we followed the suggestion of Dollase[10] and used the March formula.[11]

$$M_{hkl} = [f_{cor}\cos^2\alpha + \sin^2\alpha / f_{cor}]^{3/2} ,$$

where M_{hkl} is a corrective factor for the calculated intensity of each line; f_{cor} is a fitted coefficient which reflects the importance of preferential orientation, and α is the angle between the c axis and the hkl plane in Bragg position. The almost constant value of f_{cor} (~ 1.15), obtained for all refinements, strongly supports the validity of this correction. Using the tabulated Fermi lengths[12] and the magnetic form factor of Pr^{3+} ion taken from Ref. 13, the scaling factor f_{cor}, the silicium (germanium) atomic position $z_{Si(Ge)}$, and the magnetic moment of Pr^{3+} were refined by the MiXeD crystallographic executive for diffraction (MXD) least-squares-fit procedure.[14] The MXD program allows a simultaneous fitting of the nuclear and magnetic intensities.

The Mössbauer experiments were performed between 1.6 and 295 K. Temperatures between 1.6 and 4.2 K were controlled by pumping the helium bath through a manostat. Absorbers of 5 mg Fe/cm^2 were used in order to minimize intensity saturation effects. The source of ^{57}Co/Rh (25 mCi) was moved as a sinusoïdal or triangular function of time in synchronization with a multichannel analyzer operating in time mode. The experimental data were computer analyzed as sums of Lorentzian line shapes according to the proper physical situation.

III. BULK MAGNETIC MEASUREMENTS

Figure 2 shows the inverse susceptibility-versus-temperature curve measured in low-field values. Both compounds display a distinct minimum, indicative of antiferromagnetic ordering: $T_N = 7.70(5)$ and 14.2(1) K for $PrFe_2Si_2$ and $PrFe_2Ge_2$, respectively.

Magnetization-versus-field curves $M(H)$ at low temperature are presented in Fig. 3 for both compounds. In our available maximum field, no magnetic saturation is reached and the maximum M values of $2.43\mu_B$ (at 5 K) and $2.68\mu_B$ (at 14 K) are obtained for the Si and Ge compounds, respectively. Again, both compounds show similar low-temperature behavior typical of antiferromagnets: metamagnetic transition. For $PrFe_2Ge_2$ at 5 K, the critical field is 11 kG, in agreement with results of Ref. 5.

In the paramagnetic domain and for both compounds a slight ferromagnetic component shows up on the $M(H)$ curves. This component does not depend on temperature up to 300 K and corresponds most likely to the presence of some free-iron contamination ($< 0.5\%$ of the total iron content). Unfortunately, this is sufficient to prevent any precise determination of the effective moment values.

IV. NEUTRON-DIFFRACTION STUDY

A. Crystal structure determination

The neutron-diffraction patterns recorded in the paramagnetic state are characteristic of the nuclear scattering alone (Fig. 4). The extinction rules of the space group $I4/mmm$ are fulfilled and confirm unambiguously the $ThCr_2Si_2$-type structure for $PrFe_2Si_2$ and $PrFe_2Ge_2$. Attempts to fit the nuclear lines by inter-

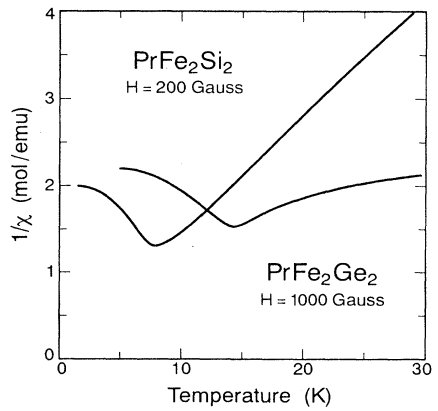

FIG. 2. Temperature dependence of the inverse molar susceptibility of $PrFe_2Si_2$ and $PrFe_2Ge_2$ in the magnetically ordered region.

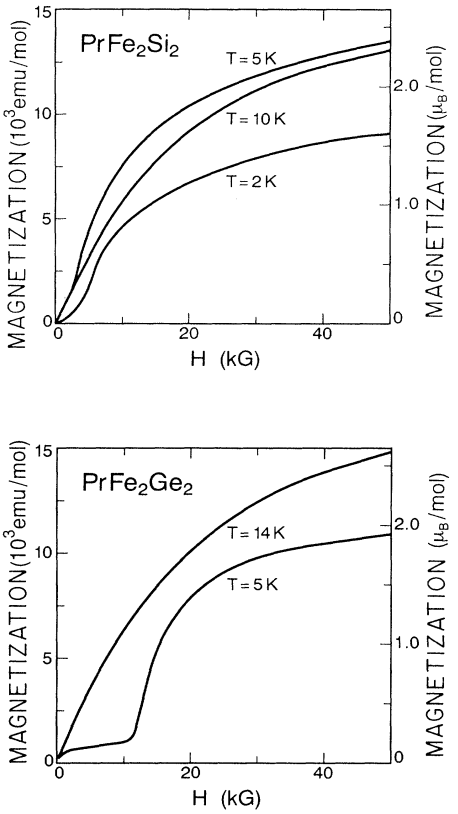

FIG. 3. Magnetic-field dependence of the magnetization of $PrFe_2Si_2$ and $PrFe_2Ge_2$ at different temperatures.

changing the positions of the Fe and Si(Ge) atoms always led to a poorer agreement and gave no evidence for any mixing between the Fe and Si(Ge) atoms in 4(*d*) and 4(*e*) sites. Comparison between the observed and calculated intensities of the nuclear peaks for each compound are given in Table II as well as the $z_{Si(Ge)}$ values, f_{cor}, the reliability factors, and the lattice parameters at $T=16$ K.

B. Magnetic structure determination

1. $PrFe_2Si_2$

Below 8 K, additional lines appear in the neutron-diffraction patterns (Fig. 4) characteristic of an antiferromagnetic ordering, in agreement with the magnetic measurements. Several superlattice lines are observed and the remaining lines are characteristic of the sole nuclear scattering with no magnetic contributions. The Bragg angles of the superlattice lines can all be indexed on the basis of a magnetic unit cell twice the chemical one by doubling the *c* axis (i.e., $a'=a$ and $c'=2c$). The absence of magnetic contribution to the (00*l*) reflections shows that the moments are aligned along the *c* axis. Analysis of the magnetic intensities suggests a simple collinear antiferromagnetic structure based on ferromagnetic (001) planes of Pr atoms with the coupling sequence (++−−). This type of magnetic ordering is usually denoted as AFII type. Table III gives the calculated and observed intensities, the adjustable parameters (z_{Si}, f_{cor}, and μ_{Pr}) and also the lattice parameters at 1.3 K.

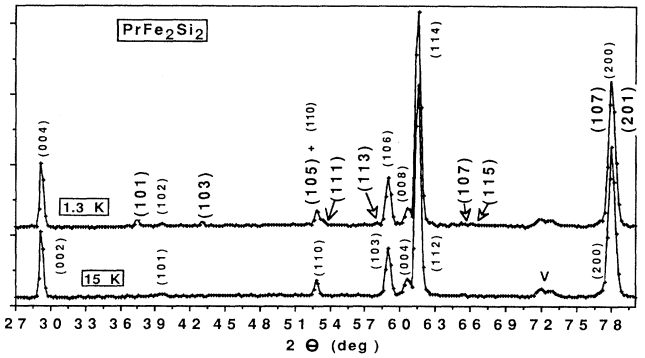

FIG. 4. Neutron-diffraction patterns of $PrFe_2Si_2$ at 15 and 1.3 K. The peaks in the ordered state are indexed on the magnetic cell by doubling the chemical cell along the *c* axis. Large size lettering denotes the magnetic reflections.

At. 1.3 K, we obtain $\mu_{Pr}=1.42(5)\mu_B$, a value which is much smaller than that expected for the theoretical Pr^{3+} free ion ($3.2\mu_B$). No localized magnetic moment on the Fe atoms was detected, within the accuracy of the neutron powder diffraction experiment.

The temperature dependence of the magnetic intensities recorded step by step between $T>T_N$ and 1.5 K (Fig. 5) gives a Pr sublattice ordering temperature $T_N=8(1)$ K in fair agreement with the bulk magnetic measurements.

TABLE II. $PrFe_2Si_2$ and $PrFe_2Ge_2$ in the paramagnetic state. Observed and calculated intensities, f_{cor}, $z_{Si(Ge)}$, lattice parameters, and reliability factors at $T=16$ K.

	$PrFe_2Si_2$			$PrFe_2Ge_2$	
hkl	I_{obs}	I_{calc}	*hkl*	I_{obs}	I_{calc}
002	241	261	002	372	369
101	17	12	101	540	533
110	170	164	110	24	18
103	694	679	103	2240	2243
004	268	258	004	98	81
112	3691	3698	112	5387	5583
200	4320	4326	200	9380	9394
$f_{cor}=1.15(4)$	$z_{Si}=0.369(3)$	$R=0.8\%$	$f_{cor}=1.16(3)$	$z_{Ge}=0.372(2)$	$R=0.3\%$
$a=4.021(1)$ Å		$c=10.029(3)$ Å	$a=4.069(1)$ Å		$c=10.475(3)$ Å

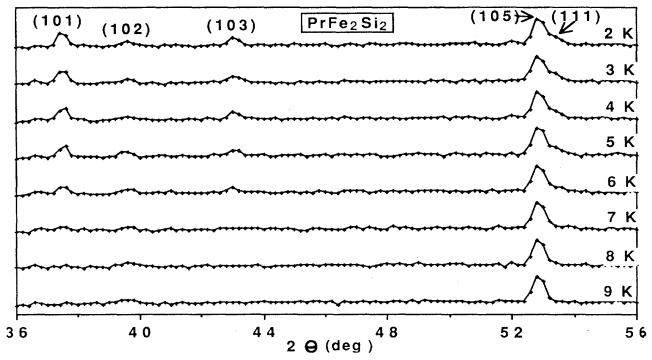

FIG. 5. Temperature dependence of the neutron-diffraction patterns of $PrFe_2Si_2$ showing the occurrence of magnetic ordering at $T_N = 8(1)$ K.

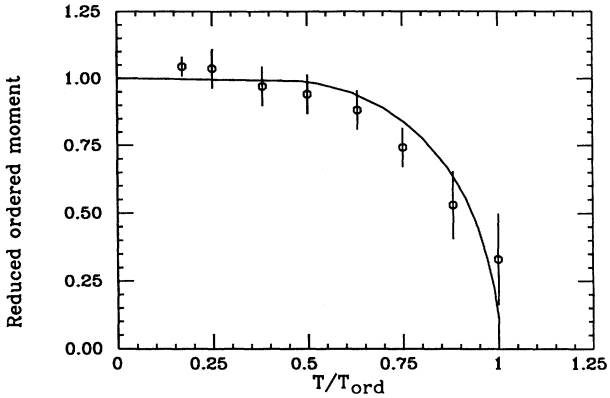

FIG. 6. Temperature dependence of the reduced ordered moment of the Pr^{3+} ions in $PrFe_2Si_2$. The solid line represents the calculated curve as obtained from the crystal-field model described in the text.

The temperature dependence of the ordered moment is shown in Fig. 6.

2. *$PrFe_2Ge_2$*

Between 14 and 9 K, the most characteristic feature of the diffractograms is the continuous variation of the angular positions of the magnetic lines with the temperature (Fig. 7), while those of the nuclear ones remain constant. The Bragg angle values of these superlattice lines are consistent with an incommensurate magnetic ordering. They may be indexed as satellites of the nuclear peaks by considering the propagation vector $Q = (0,0,q)$ and, it clearly appears that q increases (Fig. 8) slowly when the temperature decreases: $q = 0.469-0.500$ at 13 and 9 K, respectively. Except the thermal variation of Q, this result is in fair agreement with those of Szytula, Oles, and Perrin[7] and confirms the sine-modulated magnetic structure proposed by these authors (Fig. 9). It is worth noticing that in $PrFe_2Si_2$ no such thermal variation is observed in the whole range of temperature (16–1.3 K) (Fig. 8); this shows clearly that the magnetic order in

TABLE III. $PrFe_2Si_2$ and $PrFe_2Ge_2$ in the magnetic state. Observed and calculated intensities, f_{cor}, $z_{Si(Ge)}$, lattice parameters, and reliability factors at $T = 1.5$ K. The indices are given according to the magnetic cell $a' = a$, $c' = 2c$; the * is for the magnetic lines.

	$PrFe_2Si_2$			$PrFe_2Ge_2$	
hkl	I_{obs}	I_{calc}	*hkl*	I_{obs}	I_{calc}
004	1248	1266	004	474	468
101*	263	252	101*	350	351
102	69	38	102	689	672
103*	139	157	103*	240	230
110 105*	837	931	105*	141	132
111*	225	239	110	50	22
113*	221	181	111*	336	333
106	3441	3358	113* 106	2974	2981
008	1350	1240	008	136	108
114	16848	16828	114	6819	6851
107*	50	48	115*	145	176
115*	113	118	107*	75	74
201* 117* 200	20712	20526	117*	118	113
			109* 201* 200	11904	11982
$f_{cor} = 1.16(1)$	$R = 1.3\%$		$f_{cor} = 1.14(1)$		$R = 1.1\%$
$z_{Si} = 0.1824(7)$	$\mu_{Pr} = 1.42(5)\mu_B$		$z_{Ge} = 0.1868(5)$		$\mu_{Pr} = 2.75(4)\mu_B$
$a = 4.021(1)$ Å	$c = 20.052(4)$ Å		$a = 4.068(1)$ Å		$c = 20.950(6)$ Å

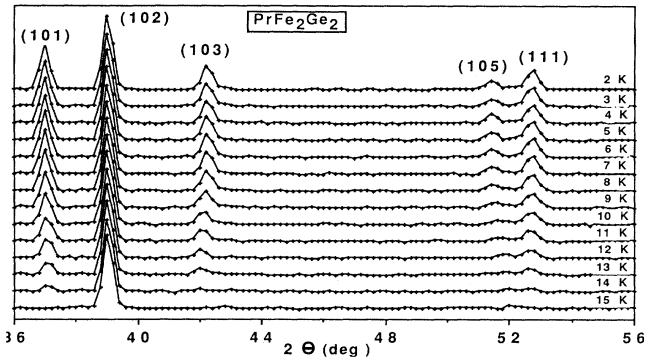

FIG. 7. Temperature dependence of the neutron-diffraction patterns of $PrFe_2Ge_2$. Note the occurrence of magnetic ordering around 14 K and the variation of the angular positions of the magnetic lines [e.g., (101)] above 9 K.

$PrFe_2Si_2$ is commensurate up to T_N.

According to Szytula, Oles, and Perrin,[7] the angular positions of all reflections remain constant from 9 K down to 1.3 K (Fig. 7), thus yielding the same magnetic ordering as the one observed in $PrFe_2Si_2$. The main difference with the study of Szytula and co-workers[7] concerns the value of the Pr magnetic moment. At 1.3 K, our refinement led to $\mu_{Pr}=2.75(4)\mu_B$ against $3.2\mu_B$ for these authors. The peculiar magnetic behavior of $PrFe_2Ge_2$ between 14 and 9 K could be considered as a progressive squaring of the sine modulation of the Pr moments which would take place in this range of temperature.

The temperature dependence of the magnetic intensities recorded step by step between $T>T_N$ and 1.5 K gives a Pr sublattice ordering temperature $T_N=14(1)$ K in fair agreement with earlier published values and our bulk magnetic measurements. The temperature dependence of the magnetic moment is given in Fig. 10.

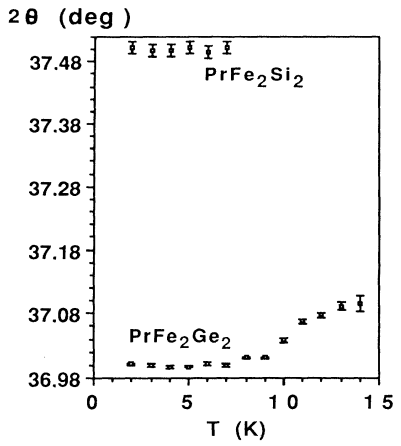

FIG. 8. Temperature dependence of the angular position of the (101) magnetic line in $PrFe_2Si_2$ and $PrFe_2Ge_2$.

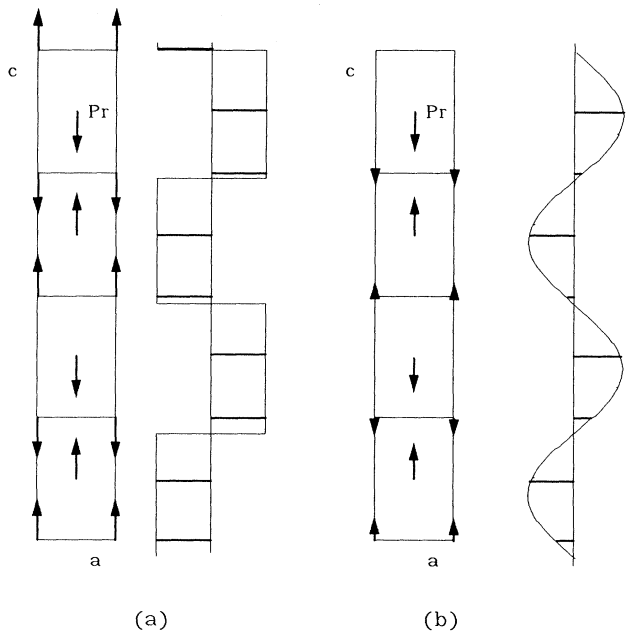

FIG. 9. Magnetic structure of $PrFe_2Ge_2$ corresponding to a complete squaring of the modulation (a). Note that it is equivalent to an AF type-II structure when $q=0.5$. (b) Incommensurate sine-modulated case.

V. MÖSSBAUER-SPECTROSCOPY STUDY

The Mössbauer study had a double aim: check the magnetic-moment difference between both compounds and confirm the kind of magnetic ordering. As a matter of fact, for an AF type-II order, we should find two iron sites with equal population: one with zero magnetic field and one experiencing a magnetic transferred field (see below). On the other hand, for an incommensurate sine-modulated structure, a magnetic-field distribution should show up as still observed in the closely related $NdFeSi_2$

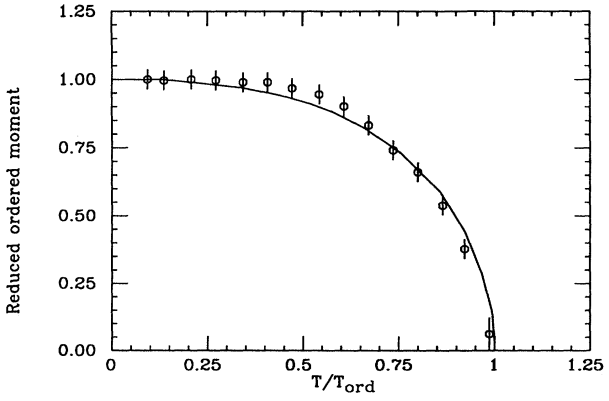

FIG. 10. Temperature dependence of the reduced ordered moment of the Pr^{3+} ions in $PrFe_2Ge_2$. The solid line represents the calculated curve as obtained from the crystal-field model described in the text.

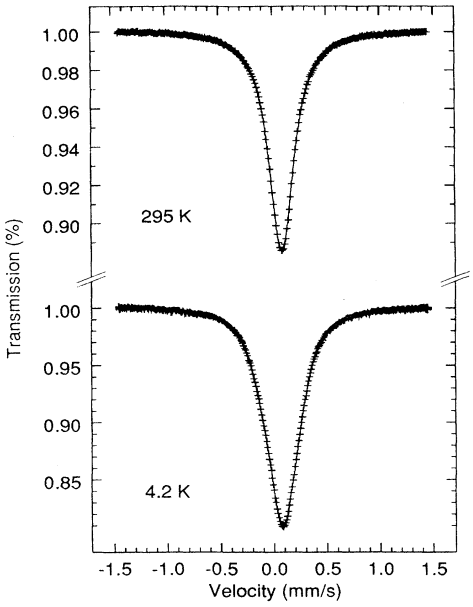

FIG. 11. ^{57}Fe-Mössbauer spectra of $PrFe_2Si_2$ at 295 K (top) and at 4.2 K (bottom). The solid curves represent the best fit to the data (see text).

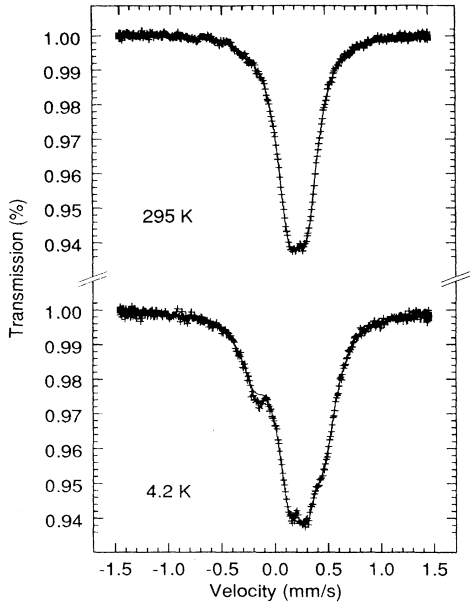

FIG. 12. ^{57}Fe-Mössbauer spectra of $PrFe_2Ge_2$ at 295 K (top) and at 4.2 K (bottom). The solid curves represent the best fit to the data (see text).

compound.[15]

^{57}Fe-Mössbauer spectra for both compounds were recorded at different temperatures between 295 and 1.55 K (Figs. 11 and 12). The Mössbauer data of $PrFe_2Si_2$ at $T > T_N$ are well represented by a single Lorentzian line whose width W, amounting to 0.280(5) mm/s at RT, is slightly larger than the value expected for a thin absorber ($\sim$0.25 mm/s). This line broadening may be attributed to unresolved quadrupolar effects ($\Delta E_Q < 0.05$ mm/s). On the other hand, poorly resolved quadrupolar split doublets are observed for $PrFe_2Ge_2$ in the paramagnetic state [$\Delta E_Q = 0.177(5)$ mm/s at RT]. The quadrupolar interactions in the $PrFe_2X_2$ intermetallics are similar to those reported in RFe_2X_2 compounds.[9,16] Their occurrence is due to the slight distortion of the Si or Ge tetrahedron surrounding the iron atoms. Indeed, for regular tetrahedra $z_{Si(Ge)} = 0.375$ and $c/a = 2\sqrt{2}$.

The isomer shifts (relative to iron metal) at 295 K of 0.193(5) and 0.318(5) mm/s for X = Si and Ge, respectively, compare well with those observed in other members of the RFe_2X_2 series.[9,16] The measurements of small positive isomer shifts is tentatively attributed to the partial filling of the iron d bands by charge transfer from the Si(Ge) atoms.[17]

TABLE IV. Hyperfine interaction parameters for ^{57}Fe in $PrFe_2Si_2$ and $PrFe_2Ge_2$ at different temperatures. δ_{IS}: isomer shift relative to iron metal at RT; $\Delta E_Q = \frac{1}{2}e^2qQ$: quadrupolar splitting; H_{hf}: hyperfine field; W: full linewidth at half maximum. The data in the ordered phase were analyzed assuming an AF type-II magnetic structure model, i.e., two iron sites A,B with relative populations $A:B = 1$ (see text).

	T (K)	δ_{IS} (mm/s)	ΔE_Q (mm/s)	H_{hf} (kOe)	W (mm/s)
$PrFe_2Si_2$	295	0.193(5)			0.280(5)
				A 9.8(2)	
	4.2	0.317(5)	$-0.031(3)^a$		0.267(3)
				B 0	
				A 10.9(2)	
	1.54	0.315(5)	$-0.035(3)^a$		0.264(3)
				B 0	
$PrFe_2Ge_2$	295	0.318(5)	0.177(5)		0.269(3)
				A 20.6(2)	
	4.2	0.437(5)	$-0.164(5)^a$		0.274(5)
				B 0	

[a] $\Delta E_Q = \frac{1}{4}e^2qQ(3\cos^2\theta - 1)$ where θ is the angle between the direction of the hyperfine field (or Pr magnetic moments) and the principal axis of the electric-field gradient which is along the c axis.

The single line observed in the paramagnetic state of $PrFe_2Si_2$ becomes significantly broadened ($W=0.36$ mm/s at 4.2 K) and non-Lorentzian in the ordered state, whereas magnetic hyperfine structure shows up clearly in the spectra of $PrFe_2Ge_2$ taken at $T<T_N$. These behaviors provide evidence for the presence of a hyperfine field at the iron nuclei due to the ordering of the Pr sublattice (Table IV).

The Mössbauer spectra of both compounds can be analyzed satisfactorily on the basis of the proposed AF type-II structure ($++--$). Assuming that the transferred fields experienced by the Fe atoms are only due to the neighboring Pr planes, it follows that the iron atoms (A) between the $++$ or $--$ layers feel a magnetic field while those (B) between the $+-$ layers experience no magnetic field.[18] The saturation fields being 10.9(2) kOe for $PrFe_2Si_2$ and 20.6(3) kOe for $PrFe_2Ge_2$ support the 1:2 ratio of the Pr magnetic moments as deduced from the neutron data. Furthermore, owing to the sizable quadrupolar interaction observed in $PrFe_2Ge_2$, the analysis of the Mössbauer data in the ordered state allows the conclusion that ΔE_Q is negative and that the Pr moments point along the c axis as expected from the neutron results. The poor spectral resolution, however, does not allow characterization of the commensurate-incommensurate transition occurring at 9 K in $PrFe_2Ge_2$.

The value of the saturation hyperfine field acting at the Fe nuclei in $PrFe_2Si_2$ deserves further comments. Its comparison to the one found in other members of the RFe_2Si_2 series[16] evidences strong departure from the simple RKKY (Ruderman-Kittel-Kasuya-Yosida) model of polarization of the conduction electrons, i.e., $H_{hf}\alpha(g_J-1)\langle J_z\rangle$. This behavior strongly suggests the occurrence of orbital polarization of the conduction band.[19]

VI. CRYSTAL-FIELD MODEL

From a structural point of view, it would be surprising that the crystal field (CF) be substantially different in $PrFe_2Si_2$ and $PrFe_2Ge_2$. In fact, we will show in the following that the observed moment ratio can be accounted for in the frame of the same CF model, with comparable splittings in the two cases, differing only in the details of the level positions at low energy.

The total Hamiltonian for the $f^2(Pr^{3+})$ configuration in tetragonal symmetry is

$$H=H_{CF}+H_{MF} , \tag{1}$$

with

$$H_{CF}=B_2^0\hat{O}_2^0+B_4^0\hat{O}_4^0+B_4^4\hat{O}_4^4+B_6^0\hat{O}_6^0+B_6^4\hat{O}_6^4 , \tag{2}$$

and

$$H_{MF}=-g_J\lambda\mu_B^2N_A\mu_{ord}\hat{J}_z , \tag{3}$$

where λ is the molecular field constant, N_A the Avogadro number (actually the number of Pr atoms per mole), and g_J the Landé g factor.

The problem of finding the CF parameters in the lack of spectroscopic measurements giving directly the transitions between the levels is a very difficult one.

On the other hand, the *ab initio* calculation of these parameters is far from being reliable, particularly in these noninsulating compounds, where there is no clear sense in assigning effective charges to the ions surrounding the rare earth. For this reason, in Ref. 20 we introduced an empirical electrostatic model (the layer model) allowing us to bypass this difficulty. This model was shown to give quite reliable values for the CF parameters in similar layered compounds.[21,22] It assumes that the main contributions to the CF on a particular R ion are due both to the tripositive ions in the same infinite plane and to the X ions in the nearest upper and lower planes. The negative effective charges Q_X on the X ions are distributed in such a way as to screen the positive charges in the R planes. This would correspond to the ideal value $Q_X=-1.5$ for perfect screening.

Now, the values of the leading parameter B_2^0 can be estimated from the Mössbauer ^{155}Gd quadrupole interaction parameters measured in the homologous $GdFe_2X_2$ compounds.[23,24] By assuming $Q(1-\gamma_\infty)=121$ b, we obtain $B_2^0=-13.5\times(1-\sigma_2)$ cm^{-1} in the Si case, and $B_2^0=-10.0\times(1-\sigma_2)$ cm^{-1} in the Ge case [the theoretical value of 0.67 (Ref. 25) will be assumed for σ_2 in the following]. These values of B_2^0 can be accounted for in the layer model by assuming $Q_X=-1.13$ and $Q_X=-1.30$ for Si and Ge, respectively, if the ionic charge of the rare earth Q_R is fixed at $+3$. In Table V, we show for both compounds the contributions to $B_2^0/(1-\sigma_2)$ (per unit of positive charge) of the various ionic planes stacked along the c axis. The nearest-neighbor contributions calculated in the frame of a point-charge model are also shown for comparison.

It appears that the only way to account for B_2^0 values close to the previous estimates is to use a strongly reduced charge Q_X with respect to the nominal ionic value $Q_X=-4$, in line with the layer model.

On the other hand, the negative sign of B_2^0 points toward a CF level scheme characterized by a singlet $\Gamma_{t1}^{(1)}$ ground state, which can lead to largely different values of μ_{ord} depending on the size of the exchange interaction and on the excitation energies of the other CF states, in particular the doublet $\Gamma_{t5}^{(1)}$ and the singlet Γ_{t2}.

Therefore, in order to have an estimate of the remaining crystal-field parameters, we fixed B_2^0 at the values obtained from electric-field-gradient measurements in the

TABLE V. Contributions to $B_2^0/(1-\sigma_2)$ in cm^{-1} and in units of positive charge.

		$PrFe_2Si_2$	$PrFe_2Ge_2$
	Pr layer	−25.7	−24.9
nn	X layers	−56.2	−49.6
nn	Fe layers	1.8	3.2
nnn	X layers	8.1	7.5
nn	Pr layers	5.0	4.9
nn	Pr ions	−12.6	−12.2
nn	X ions	−31.5	−26.1
nn	Fe ions	40.7	39.1

TABLE VI. CF parameters (in cm^{-1}) calculated after layer model, assuming $Q_X=-1.13$ (Si) and -1.30 (Ge) with $Q_R=+3$ (see text).

	$B_4^0\times10$	$B_6^0\times10^3$	B_4^4	$B_6^4\times10^3$
$PrFe_2Si_2$	0.210	0.211	0.406	−0.633
$PrFe_2Ge_2$	0.249	0.222	0.392	−0.969

homologous Gd compounds. The B_4^m and B_6^m parameters ($m=0,4$) were calculated in the frame of the layer model by assuming $Q_X=-1.13$ and $Q_X=-1.30$ for Si and Ge, respectively, with $Q_R=+3$. Table VI shows the calculated values for B_4^m and B_6^m.

Starting from the values of the five CF parameters determined in this way, we can calculate the energy levels, which are given in Table VII. Both compounds are characterized by the presence of the excited Γ_{t2} singlet at about 15 cm^{-1}. The $\Gamma_{t5}^{(1)}$ doublet lies between the two lowest singlets in the Ge compound, while it is higher than the two singlets in the Si compound. The remaining four states are quite enhanced in energy with respect to the first group of three. The overall splitting is ~190 and ~240 cm^{-1} in the two cases, respectively. If we calculate self-consistently the ordered moment at $T=0$,[21] we obtain $\mu_{ord}=2.75\mu_B$ for the Ge case and $\mu_{ord}=1.65\mu_B$ for the Si case. Therefore, the essential aspect of the magnetic behavior of the two compounds is correctly described in the frame of this raw model. A further refinement can be obtained by observing that the details of the level positions in the lowest group can be changed significantly by small variations of the higher-order parameters. In particular, in the Ge case, the lowest doublet is too close to the ground singlet to account for the low-temperature behavior of the magnetization curve as obtained by neutron scattering (Fig. 10). In fact, with the level configuration in Table VII (upper line) the value of μ_{ord} at $T=0$ would decrease of about 10% by increasing the temperature of only 1 K. We can easily enhance the value of the doublet excitation energy by the same method used in Ref. 26, adapted for the different ground state. This leads to a slight modification of $B_4^0=0.213\times10^{-1}$ and $B_6^0=0.187\times10^{-3}$ cm^{-1}. With these values, the ordered moment is $2.66\mu_B$ at $T=0$ and goes to zero at $T_N=14$ K.

As regards the Si case, an ordered moment of $1.51\mu_B$ at $T=0$ can be easily accounted for self-consistently with $T_N=7.6$ K by increasing the B_4^4 value by a few percent, $B_4^4=0.420$ cm^{-1}.

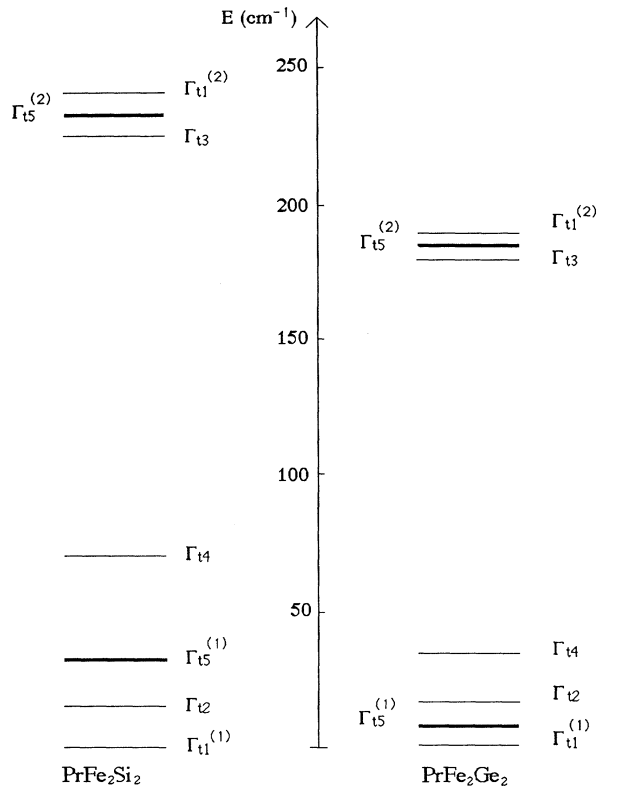

FIG. 13. Crystal-field level schemes in the paramagnetic state of $PrFe_2Si_2$ and $PrFe_2Ge_2$ as obtained from the modified layer model (see text).

The energy-level scheme corresponding to these new CF parameters is given in Table VII (lower line) and Fig. 13.

The calculated behavior of the magnetization is shown in Figs. 6 and 10 for the Si and the Ge case, respectively, and compared with the experimental behavior. Reduced units have been used along both temperature and ordered moment axes, to show better the quality of the agreement. The small discrepancies between the calculated and experimental values of T_N and of μ_{ord} at $T=0$ are not significant, taking into account the approximations of the model.

The level schemes we have proposed come out essentially from the empirical layer model. However, it is possible to show in a more general way that the possible solutions for the CF problem, accounting for the experi-

TABLE VII. Calculated CF energy levels (in cm^{-1}) according to initial and (modified) layer model (see text).

	$\Gamma_{t1}^{(1)}$	Γ_{t2}	$\Gamma_{t5}^{(1)}$	Γ_{t4}	Γ_{t3}	$\Gamma_{t5}^{(2)}$	$\Gamma_{t1}^{(2)}$
$PrFe_2Si_2$	0	13.4	33.1	72.4	222	231	239
		(14.3)	(32.6)	(70.7)	(225)	(233)	(241)
$PrFe_2Ge_2$	0	15.3	1.3	29.4	175	182	189
		(15.2)	(8.8)	(34.0)	(180)	(184)	(189)

TABLE VIII. Alternative parameters describing the CF Hamiltonian of the $PrFe_2X_2$ compounds (see text).

	x	B_2^0 (cm^{-1})	Δ (cm^{-1})	ϵ
$PrFe_2Si_2$	0.9925	−4.45	14.3	0.686
$PrFe_2Ge_2$	0.9878	−3.32	15.2	0.678

mental values of both T_N and μ_{ord}, are very close to those given in Table VII (lower line) and Fig. 13.

In fact, we are able to treat the problem of the $J=4$ multiplet in tetragonal symmetry, allowing for a ground state of the $\Gamma_{t1}^{(1)}$ type, by imposing from the beginning some external conditions, directly available from the experiments, which have to be satisfied by the model. This can be done in the same way as in Ref. 26 for the case of the $\Gamma_{t5}^{(1)}$ ground state. For the singlet ground state we have extended the model in Ref. 21 to take into account all the CF levels in the split $J=4$ multiplet. The details of this approach will be described elsewhere.[27] The central point is that we can introduce an alternative parametrization for the CF Hamiltonian, which has a more intuitive physical meaning and allow us to select only the solutions for the CF parameters which are compatible with the given values of T_N and μ_{ord}.

These solutions depend on the four parameters $(x, B_2^0, \Delta, \epsilon)$, x being the Lea, Leask, and Wolf (LLW) (Ref. 28) parameter characterizing the cubic part of the Hamiltonian.[26] Δ is the splitting between Γ_{t2} and $\Gamma_{t1}^{(1)}$ and ϵ the coefficient of the $(|4\rangle+|-4\rangle)$ component of the ground wave function.

These parameters are shown in Table VIII for the case corresponding to the modified layer model results of Table VII, and for both compounds.

Within a physically reasonable range for the total splitting (namely, $\Delta_{tot}<400$ cm^{-1}) and by fixing B_2^0 at the value quoted above, we have found solutions in the Si case only for $x>0.95$ and $9.65<\epsilon<0.70$. The value of Δ can range from 15 to 45 cm^{-1}, but the solutions tend to move to higher values of x at higher energy.

In the Ge case, we observe the same trend, although at $\Delta\sim35$ cm^{-1} the solutions already disappear. However, other possible solutions appear at $\Delta\sim20$ cm^{-1}, with ϵ ranging from ~0.18 to ~0.32. They always move to higher x values with increasing Δ. Evidently, a higher value of μ_{ord} can be obtained easily within this level scheme.

What is clear is that the only range of parameters accounting for the principal magnetic features of both compounds is the same as the one obtained by the layer model. If neutron inelastic scattering experiments confirm the proposed level scheme, we should then be able to speculate on the reasons of this fact and on the ability of the model to give deeper insight on the CF effects in compounds of the same family.

VII. CONCLUSIONS

The $PrFe_2X_2$ (X=Si, Ge) intermetallic compounds exhibit antiferromagnetic ordering of the Pr sublattice at 7.70 and 14.2 K, respectively. Neutron and Mössbauer experiments show than an AF type-II (++−−) structure, as observed in the isotypic $NdFe_2Si_2$ compound,[7] occurs at low temperature in $PrFe_2Si_2$ and $PrFe_2Ge_2$. In both cases, the c axis is the easy direction of the Pr moments. This is in agreement with the negative sign of B_2^0 inferred from the ^{155}Gd quadrupolar interaction data in the parent $GdFe_2X_2$ compound.[23,24] No local moment was detected on the iron site. It is interesting to note that the stabilization of a simple collinear AF ordering, in both compounds at 1.3 K, agrees with the systematics based on the a/c values [i.e., oscillatory magnetic ordering is expected to appear only if $a/c>1\sqrt{6}=0.4082$ (Ref. 3)]. However, in $PrFe_2Ge_2$ an additional incommensurate-commensurate (IC) transition towards a sine-wave spin structure shows up at $T_{IC}=9$ K. As discussed previously,[29] the ANNNI (anisotropic next-nearest-neighbor Ising model), suitable for layered compounds, may explain the stabilization of the AF type-II structure as well as the IC transition observed at higher temperatures in $PrFe_2Ge_2$. The occurrence of quite different saturation Pr moments in $PrFe_2Si_2$ ($1.41\mu_B$) and in $PrFe_2Ge_2$ ($2.75\mu_B$) as inferred from the neutron data and confirmed by ^{57}Fe-Mössbauer measurements is explained straightforwardly in the frame of an empirical electrostatic crystal-field model (the so-called layer model). It is shown that the relative position of the crystal field $\Gamma_{t5}^{(1)}$ doublet (lying between the two lowest singlets in the Ge compound) plays a central role on the actual value of the ordered moments in the $PrFe_2X_2$ compounds. In the frame of this model we deduced a complete set of crystal-field parameters (B_2^0, B_4^m, and B_6^m, where $m=0,4$) suitable to reproduce both the values of the ordered moments and their temperature dependences. The proposed CF level schemes in $PrFe_2X_2$ compounds will be checked by inelastic neutron scattering and specific-heat measurements in the near future.

ACKNOWLEDGMENTS

Neutron-diffraction data were recorded at the Institut Laüe Langevin (ILL). We are grateful to J. L. Soubeyroux, responsible for the spectrometer used, for his help during the measurements. We are very indebted to P. Santini for his assistance in the computation of the CF parameters. Laboratoire de Chimie du Solide Minéral is Unité Associée au CNRS No. 158.

[1] E. Parthé and B. Chabot, in *Handbook on the Physics and Chemistry of Rare Earths*, edited by K. A. Gschneider, Jr. and L. Eyring (North-Holland, Amsterdam, 1984), Vol. 6, p. 113.

[2] P. Rogl, in *Handbook on the Physics and Chemistry of Rare Earths*, edited by K. A. Gschneider, Jr. and L. Eyring (North-Holland, Amsterdam, 1984), Vol. 7, p. 1.

[3] A. Szytula and J. Leciejewicz, in *Handbook on the Physics and*

Chemistry of Rare Earths, edited by K. A. Gschneider, Jr. and L. Eyring (North-Holland, Amsterdam, 1989), Vol. 12, p. 133.

[4]I. Felner, I. Mayer, A. Grill, and M. Schieber, Solid State Commun. **16**, 1005 (1975).

[5]J. Leciejewicz, A. Szytula, and A. Zygmunt, Solid State Commun. **45**, 149 (1982).

[6]A. Szytula, W. Bazela, and J. Leciejewicz, Solid State Commun. **48**, 1053 (1983).

[7]A. Szytula, A. Oles, and M. Perrin, J. Magn. Magn. Mater. **86**, 377 (1990).

[8]H. Pinto and H. Shaked, Phys. Rev. B **7**, 3261 (1973).

[9]J. J. Bara, H. U. Hrynkiewicz, A. Milos, and A. Szytula, J. Less-Common Met. **161**, 185 (1990).

[10]W. A. Dollase, J. Appl. Crystallogr. **19**, 267 (1986).

[11]A. March, Z. Kristallogr. Kristallogeom. Krystallphys. Kristallchem. **81**, 285 (1932).

[12]V. F. Sears (unpublished).

[13]C. Stassis, H. W. Deckmann, B. N. Harmon, J. P. Desclaux, and A. J. Freeman, Phys. Rev. B **15**, 369 (1977).

[14]P. Wolfers, J. Appl. Crystallogr. **23**, 554 (1990).

[15]B. Malaman, G. Venturini, G. Le Caer, L. Pontonnier, D. Fruchart, K. Tomala, and J. P. Sanchez, Phys. Rev. B **41**, 4700 (1990).

[16]D. R. Noakes, A. M. Umarji, and G. K. Shenoy, J. Magn. Magn. Mater. **39**, 309 (1983).

[17]J. D. Cashion, G. K. Shenoy, D. Niarchos, P. J. Viccaro, and C. M. Falco, Phys. Lett. A **79**, 454 (1980).

[18]A. M. Umarji, D. R. Noakes, P. J. Viccaro, G. K. Shenoy, A. T. Aldred, and D. Niarchos, J. Magn. Magn. Mater. **36**, 61 (1983).

[19]B. D. Dunlap, I. Nowik, and P. M. Levy, Phys. Rev. B **7**, 4232 (1973).

[20]B. Malaman, G. Venturini, A. Blaise, G. Amoretti, and J. P. Sanchez, J. Magn. Magn. Mater. **104-107**, 1359 (1992).

[21]G. Amoretti, A. Blaise, and J. Mulak, J. Magn. Magn. Mater. **42**, 65 (1984).

[22]G. Amoretti, A. Blaise, P. Burlet, J. E. Gordon, and R. Troc, J. Less-Common Met. **121**, 233 (1986).

[23]G. Czjzek, V. Oestreich, H. Schmidt, K. Latka, and K. Tomala, J. Magn. Magn. Mater. **79**, 42 (1989).

[24]I. Felner and I. Nowik, J. Phys. Chem. Solids **39**, 767 (1978).

[25]R. M. Sternheimer, M. Blume, and R. F. Peierls, Phys. Rev. **173**, 376 (1968).

[26]G. Amoretti, A. Blaise, R. Caciuffo, J. M. Fournier, J. Larroque, and R. Osborn, J. Phys. Condens. Matter **1**, 5711 (1989).

[27]G. Amoretti, P. Santini, A. Blaise, and R. Caciuffo, J. Appl. Phys. (to be published).

[28]K. R. Lea, M. J. M. Leask, and W. P. Wolf, J. Phys. Chem. Solids **23**, 1381 (1962).

[29]J. Rossat-Mignod, in *Neutron Scattering in Condensed Matter Research,* Methods of Experimental Physics, Part C, edited by K. Sköld and D. L. Price (Academic, New York, 1987) Vol. 23, p. 69.